Multicopper oxidase-1 is a ferroxidase essential for iron homeostasis in *Drosophila melanogaster*

Minglin Lang, Caroline L. Braun, Michael R. Kanost, Maureen J. Gorman

Published Version Information

Citation: Lang, M., Braun, C. L., Kanost, M. R., & Gorman, M. J. (2012). Multicopper oxidase-1 is a ferroxidase essential for iron homeostasis in *Drosophila melanogaster*. Proceedings of the National Academy of Sciences of the United States of America, 109(33), 13337-13342.

Digital Object Identifier (DOI): doi:10.1073/pnas.1208703109

Publisher's Link: http://www.pnas.org/content/109/33/13337.full

Multicopper oxidase-1 is a ferroxidase essential for iron homeostasis in *Drosophila melanogaster*

Minglin Lang[1,2], Caroline L. Braun[1], Michael R. Kanost[1], Maureen J. Gorman[1,*]

[1]Department of Biochemistry, Chalmers Hall, Kansas State University, Manhattan, Kansas, USA
[2]College of Life Science, Lekai South Street, Agricultural University of Hebei, Baoding, China

*Corresponding author:

Maureen Gorman
141 Chalmers
Department of Biochemistry
Kansas State University
Manhattan, KS 66506
U.S.A.
Tel 1-785-532-6922
Fax 1-785-532-7278
mgorman@ksu.edu

classification: Biological Sciences, genetics

Abstract

Multicopper ferroxidases catalyze the oxidation of ferrous iron to ferric iron. In yeast and algae, they participate in cellular uptake of iron; in mammals, they facilitate cellular efflux. The mechanisms of iron metabolism in insects are still poorly understood, and insect multicopper ferroxidases have not been identified. In this paper we present evidence that *Drosophila melanogaster* multicopper oxidase-1 (MCO1) is a functional ferroxidase. We identified candidate iron binding residues in the MCO1 sequence and found that purified recombinant MCO1 oxidizes ferrous iron. An association between MCO1 function and iron homeostasis was confirmed by two observations: RNAi-mediated knockdown of MCO1 resulted in decreased iron accumulation in midguts and whole insects, and weak knockdown increased the longevity of flies fed a toxic concentration of iron. Strong knockdown of MCO1 resulted in pupal lethality, indicating that *MCO1* is an essential gene. Immunohistochemistry experiments demonstrated that MCO1 is located on the basal surfaces of the digestive system and Malpighian tubules. We propose that MCO1 oxidizes ferrous iron in the hemolymph and that the resulting ferric iron is bound by transferrin or melanotransferrin leading to iron storage, iron withholding from pathogens, regulation of oxidative stress and/or epithelial maturation. These proposed functions are distinct from those of other known ferroxidases Given that MCO1 orthologs are present in all insect genomes analyzed to date, this discovery is an important step toward understanding iron metabolism in insects.

Introduction

Multicopper ferroxidases catalyze the oxidation of ferrous iron (Fe^{2+}) to ferric iron (Fe^{3+}). Redox cycling between the two oxidation states is a critical aspect of iron metabolism because the two forms of iron have different properties: ferrous iron is soluble under most physiological conditions, but it participates in toxic radical formation, whereas ferrric iron does not promote radical formation, but it is highly insoluble [1]. Multicopper ferroxidases in yeast and algae function in the uptake of iron by oxidizing ferrous to ferric iron, which is then transported into the cell by a ferric iron permease [2, 3]. The mammalian ferroxidases, hephaestin and ceruloplasmin, facilitate iron efflux by oxidizing extracellular ferrous iron that has been transported out of cells by a ferrous iron permease (ferroportin) [4, 5]. Hephaestin is bound to the basolateral membrane of intestinal cells, thus, a reduction in hephaestin function leads to an accumulation of iron in the intestinal cells and a deficiency of iron in the rest of the body [6]. A decrease in the function of ceruloplasmin (which is expressed as circulating and GPI-anchored isoforms) leads to an overaccumulation of iron in many tissues due to a decrease in iron efflux [7].

Iron metabolism in insects is not well understood, but some components of the iron metabolism pathways are known. Divalent metal transporter 1 (DMT1) transports iron from the diet into midgut epithelial cells [8]. Ferritin has two functions in insects: iron storage (comparable to the function of mammalian ferritin) and iron transport [9]. Insect ferritin is present in the endoplasmic reticulum and Golgi complex of a variety of cell types, including midgut cells, and iron-loaded ferritin is secreted into the hemolymph and is thought to transport iron to other parts of the body [9]. Insect transferrin is present in the hemolymph, and, like mammalian transferrin, it may function as an iron transport protein [10, 11], although the mechanism of ferric-transferrin uptake is unknown [12]. We wondered whether iron metabolism in insects requires the activity of a multicopper ferroxidase. Given that ferroxidases are necessary for iron metabolism in a diverse set of organisms [2, 3, 6, 7, 13, 14], it seemed likely that they would exist in insects. On the other hand, the multicopper ferroxidases with known physiological functions work in conjunction with an iron permease [2-5], whereas we and others have been unable to identify an iron permease gene in any insect genome [9].

To identify candidate insect ferroxidases, we evaluated the known set of insect multicopper oxidases (MCOs) [15]. In addition to multicopper ferroxidases, the MCO family of enzymes includes laccases, which oxidize a broad range of substrates (including diphenols), ascorbate oxidases, which oxidize ascorbate, and a few less common oxidoreductases [16]. All insect genomes analyzed to date contain at least two MCO genes, *MCO1* and *MCO2*, and some insect species have more, for example, the *Drosophila melanogaster* genome encodes four [15]. MCO1 orthologs have unknown enzymatic and physiological functions [15]. MCO2 orthologs are laccases that participate in pigmentation and sclerotization of newly synthesized cuticle [15]. *D. melanogaster* MCO3, which has no known orthologs outside of Drosophilidae, is predicted to be a ferroxidase because it contains a putative iron binding residue, and loss of function leads to an increase in iron accumulation in the midgut; however, evidence of

ferroxidase activity and information about when and where *DmMCO3* is expressed are not available [8]. Because MCO2 orthologs are known to be laccases, and most other insect MCOs, including DmMCO3, are found in only a subset of insect species, we decided to focus on MCO1.

The goal of this study was to determine whether MCO1 functions as a ferroxidase. Previous studies of gene expression in *D. melanogaster* found that *MCO1* mRNA is most abundant in late stage embryos, feeding stage larvae, and adults, and that *MCO1* is expressed predominantly in the digestive system (midgut, hindgut and crop) and Malpighian tubules [17, 18]. These expression profiles are similar to those of *MCO1* orthologs in *Anopheles gambiae* and *Manduca sexta* [19-21]. To establish whether MCO1 functions as a ferroxidase in *D. melanogaster*, we purified recombinant MCO1 and analyzed its enzymatic activity, performed immunohistochemistry to determine the location of MCO1 within the insect, and evaluated the loss-of-function phenotypes generated by RNAi-mediated knockdown.

Results and Discussion

MCO1 orthologs have putative iron binding residues

A typical MCO consists of three cupredoxin-like domains, and residues in domains II and III form the substrate binding pocket [22, 23]. Multicopper ferroxidases have conserved acidic residues that bind to ferrous iron, for example, the substrate binding site of a yeast ferroxidase, Fet3p, has three acidic residues that coordinate iron binding: Glu185, Asp283 and Asp409 [24, 25]. To identify possible iron binding residues in MCO1, we aligned the *D. melanogaster* MCO1 sequence with the Fet3p sequence. Two acidic residues in the MCO1 cupredoxin-like domain II, Asp380 and Glu552, align with Glu185 and Asp283 in Fet3p (Figures S1 and S2). We verified that these two acidic residues are conserved in MCO1 orthologs from other insect species (Figure S1). Given the high degree of conservation of these residues in MCO1 orthologs and given that Asp409 is not required for the ferroxidase activity of Fet3p [25], we hypothesized that MCO1 functions as a ferroxidase.

MCO1 has ferroxidase activity

To allow us to directly investigate the enzymatic activity of MCO1, we expressed a recombinant form of the enzyme in cultured insect cells. The MCO1 sequence contains a predicted signal peptide, two von Willebrand factor domains, a cysteine rich region, three cupredoxin-like domains, and a putative carboxyl-terminal transmembrane segment (Figure S2). Expression and purification of the full-length, wild-type protein was difficult due to low expression and proteolytic cleavage. To circumvent these problems, we expressed recombinant MCO1 without the von Willebrand factor domains and transmembrane segment, and we mutated Arg454 to alanine to reduce proteolytic cleavage (Figure S2). The secreted enzyme was purified from serum-free medium with the use of lectin affinity, anion exchange and size exclusion chromatography. The

identity of the purified enzyme was confirmed by immunoblot analysis, and adequate purity was verified by SDS-PAGE followed by Coomassie staining (Figures 1 and S2).

Multicopper ferroxidases oxidize laccase substrates in addition to ferrous iron, but usually at a much lower catalytic efficiency [24]. To analyze the substrate preferences of MCO1, we compared the activity of recombinant MCO1 with that of two mosquito laccases, *Anopheles gambiae* MCO2A and MCO3 [26, 27]. We determined kinetic constants associated with four laccase substrates, including a *p*-diphenol (hydroquinone) and three *o*-diphenols that are natural substrates of insect laccases (dopamine, *N*-acetyldopamine (NADA) and *N*-β-alanyldopamine (NBAD) [26]). We found that MCO1 had detectable laccase activity; however, the catalytic efficiencies (k_{cat}/K_m) were much lower than those of MCO2A and MCO3 (Table 1). These results suggest that MCO1 does not function as a laccase *in vivo*. To determine whether MCO1 has ferroxidase activity, an in-gel assay was used. Of the three enzymes, only MCO1 had detectable ferroxidase activity (Figure 1). These results suggest that MCO1 functions as a ferroxidase.

MCO1 is present on the basal surface of the digestive system and Malpighian tubules

To verify expression of *MCO1* in the midgut and Malpighian tubules and to determine whether *MCO1* expression is affected by the concentration of iron in the flies' diet, we used quantitative RT-PCR to analyze *MCO1* transcript abundance in whole flies, midguts and Malpighian tubules. Flies were fed regular food or food supplemented with 0.5 mM or 10 mM iron. We found that iron supplementation had no detectable effect on *MCO1* expression in whole flies, midguts or Malpighian tubules (Figure S3). Based on its amino acid sequence, we would expect MCO1 to enter the secretory pathway in cells of the midgut and Malpighian tubules and to remain attached to the cell membrane by a carboxyl-terminal transmembrane segment. Immunostaining supports this prediction. MCO1 immunoreactivity was along the basal surface of the midgut and Malpighian tubules (Figures 2 and S4). Immunostaining was not restricted to particular regions of the digestive system or Malpighian tubules (Figure S4). The basal location of MCO1 immunoreactivity suggests that MCO1 is extracellular and, thus, positioned to oxidize ferrous iron in the hemolymph.

Knockdown of MCO1 is correlated with increased longevity on high iron food and decreased iron accumulation

To detect *MCO1* loss-of-function phenotypes, we used RNAi-mediated knockdown. Strong knockdown was accomplished by crossing an *actin-Gal4* (*act-Gal4*) driver line with a *UAS-dsMCO1* responder line; weak knockdown was achieved with a *daughterless-Gal4* (*da-Gal4*) driver. Negative controls were produced by crossing the driver with a line that is genetically similar to the RNAi line except for the lack of a *dsMCO1* transgene. Knockdown was verified by quantitative RT-PCR (Figure S5). We found that strong knockdown of MCO1 resulted in pupal lethality. In contrast, insects with a weak knockdown of MCO1 survived to adulthood, and they lived as long as

negative controls (Figure 3). The lethality associated with strong knockdown indicates that *MCO1* is an essential gene.

If MCO1 is involved in iron metabolism, we might expect knockdown to affect the longevity of flies cultured on food with a toxic concentration of iron. To test this hypothesis, we cultured *da-Gal4>UAS-dsMCO1a* and *da-Gal4>attP* (control) flies on food supplemented with 10 mM ferrous ammonium citrate, a concentration of iron that decreased longevity in control flies (Figure 3). We found that MCO1 knockdown flies lived significantly longer than control flies on the iron supplemented food (Figure 3), indicating that knockdown of MCO1 protects the flies from iron toxicity.

Diminished iron accumulation in knockdown insects would provide an explanation for protection against iron toxicity. We used two methods to test the hypothesis that MCO1 knockdown leads to less iron accumulation: a histological method to detect iron in the midgut [29], and a ferrozine-based assay to estimate the iron content of whole insects [30]. Both methods demonstrated a correlation between knockdown of MCO1 and a decrease in iron accumulation (Figures 4, 5 and S6). The decreased iron content in knockdown insects demonstrates that iron accumulation is influenced by MCO1 function.

Possible functions of MCO1

The apparent absence of MCO1 on the apical surface of midgut epithelial cells argues against a role for MCO1 in the uptake of iron from the diet. The presence of MCO1 on the basal surface of midgut cells suggests a possible hephaestin-like function (i.e., a role in iron efflux from intestinal cells [6]). In support of this hypothesis is the observation that loss of MCO1 function is correlated with a decrease in whole body iron content. On the other hand, knockdown of MCO1 resulted in less midgut iron, not the overaccumulation observed in mammalian hephaestin mutants. In addition, since hephaestin functions together with an iron permease, whereas no insect iron permease has been identified, if MCO1 contributes to iron efflux from midgut cells, its mechanism is likely to differ from that of hephaestin. One explanation for the decrease in iron accumulation is an unidentified feedback mechanism. For example, knockdown of MCO1 may result in an excess of ferrous iron in the hemolymph, which may act as a signal to downregulate iron uptake from the diet. If this explanation is correct, we might expect knockdown of MCO1 to lead to a downregulation of *DMT1* and a corresponding decrease in iron transport from the gut lumen to the midgut epithelial cells. As an initial test of this hypothesis, we used quantitative RT-PCR to analyze *DMT1* expression and found that knockdown of MCO1 did result in lower *DMT1* transcript abundance in the midgut (Figure 6).

As mentioned above, the basal location of MCO1 suggests that the enzyme is positioned to oxidize ferrous iron to ferric iron in the hemolymph. The resulting ferric iron could be loaded onto transferrin and transported to iron deficient cells for uptake, as is the case in mammals [31]. Alternatively, oxidation of ferrous iron followed by transferrin loading may play a protective role by limiting toxic radical formation, which is generated by ferrous but not ferric iron [1], or, it may have an immune function, given that ferric-

transferrin is less likely than free iron to serve as a source of iron for pathogens [32]. The possibility of an immune function is supported by upregulation of *MCO1* in *D. melanogaster* [33] and *A. gambiae* [19] in response to infection. Finally, the oxidation of ferrous iron by MCO1 may supply ferric iron to melanotransferrin, which is required for septate junction formation during epithelial maturation in *D. melanogaster* [34]. A developmental role for MCO1 would provide an explanation for the pupal lethality caused by strong MCO1 knockdown.

Conclusion

The main goal of this study was to determine whether MCO1 functions as a ferroxidase. Several lines of evidence indicate that it does: presence of putative iron binding residues in cupredoxin-like domain II, ferroxidase activity of recombinant MCO1, increased longevity of knockdown flies (compared with control flies) when cultured on high iron food, and decreased iron accumulation in knockdown insects. In addition, we determined that MCO1 is located on the basal surfaces of the digestive system and Malpighian tubules. We propose the following hypothetical model: MCO1 oxidizes ferrous iron in the hemolymph, and the resulting ferric iron is bound by transferrin or melanotransferrin leading to iron storage, iron withholding from pathogens, regulation of oxidative stress and/or epithelial maturation. Given that MCO1 orthologs have been identified in all insect genomes analyzed to date, our discovery that DmMCO1 is a ferroxidase should lead to a better understanding of iron metabolism in a wide range of insect species, including blood-feeding insects such as mosquitoes, which ingest a large amount of iron with each blood meal. Now that many of the components of the iron metabolism pathways in insects and mammals have been identified and studied, a picture of two distinct systems for metabolizing iron has emerged. Although the pathways in insects and mammals have many of the same elements (e.g., DMT1, ferritins, transferrins and multicopper ferroxidases), some components that are critical in mammals, such as ferroportin and transferrin receptor, may not exist in insects, and even some of the homologous proteins, including multicopper ferroxidases, seem to have divergent functions. It is interesting to consider that insects (with their open circulatory system) and mammals (with their need for large amounts of iron-bound hemoglobin) may have evolved to metabolize iron differently.

Materials and methods

Sequence analyses

Sequence alignments and analyses were performed as described previously [27]. The GenBank ID for each sequence analyzed is listed in Table S1.

Recombinant protein expression

A full length *MCO1* cDNA was obtained from the Drosophila Genomics Resource Center (Bloomington, Indiana). This clone (RE34633) had a Gly331Ser mutation, which was

reversed with site-directed mutagenesis using the QuickChange Multi Site-Directed Mutagenesis Kit (Stratagene). Expression and purification of the full-length, wild-type protein was difficult due to low expression and proteolytic cleavage. To circumvent these problems, we generated a truncated cDNA that encoded only the cysteine-rich region and cupredoxin-like domains (Figure S2), cloned it in-frame with the *D. melanogaster* Bip signal sequence from the pMT/Bip/V5/His vector (Invitrogen), and used site-directed mutagenesis to create an Arg454Ala mutant that was less susceptible to proteolytic cleavage. This cDNA was cloned into the pOET3 vector and the flashBAC system (Oxford Expression Technologies) was used to generate a recombinant baculovirus. Expression in Sf9 cells and purification by concanavalin-A-Sepharose and Q-Sepharose were done as described previously [27]. Additional purification was accomplished with the use of a Superdex 200 HiLoad 16/60 column (GE Healthcare Life Sciences). The concentration of purified recombinant MCO1 was estimated as described previously [27]. The yield was approximately 0.5 mg MCO1 per liter of cell culture.

Activity assays

Laccase activity assays, determination of pH optima, and calculation of kinetic constants were performed as described previously [26]. Briefly, reactions were done by mixing 0.5 μg MCO1 with substrate in a total volume of 200 μl and detecting product formation with a microplate spectrophotometer by observing the change in absorbance over time. All assays were done in triplicate. MCO1 had the highest activity at pH 6.0-8.0; therefore, pH 7.0 was used for determining kinetic constants. Ferroxidase activity was assayed with an in-gel method [27]. Ten μg recombinant MCO1, *A. gambiae* MCO2A [26] and *A. gambiae* MCO3 [27] were subjected to native PAGE in triplicate; one gel was stained with Coomassie blue, another was incubated in 9.2 mM *p*-phenylenediamine (Sigma) to detect laccase activity, and a third gel was incubated in 0.2 mM ferrous ammonium sulfate followed by a brief incubation with 15 mM FerroZine (Acros Organics) to detect ferroxidase activity.

Drosophila culture and genetics

Flies were cultured at 25°C on K12 High Efficiency diet (USBiological) unless otherwised noted. Two ubiquitous *Gal4* driver stocks were obtained from the Bloomington Drosophila Stock Center at Indiana University (BDSC): y^1 *w*; *act-Gal4*/ *CyO* (#25374), and w^{1118}; *da-Gal4* (#8641). A gut/salivary gland specific *Gal4* driver line (*mg+sg-Gal4*) was obtained from the Drosophila Genetics Resource Center in Kyoto: w^*; *P{w[+mW.hs]=GawB}NP3084* (#113-094). Two RNAi lines were obtained from the Vienna Drosophila RNAi Center (VDRC): w^{1118}; *UAS-dsMCO1a*/ *CyO* (#108677 from the KK library), and w^{1118}; *UAS-dsMCO1b* (#15602 from the GD library). The two RNAi lines have insertions at different chromosomal locations, target different regions of the *MCO1* mRNA, and are predicted to have no off-targets. *UAS-dsMCO1a* is inserted into an *attP* site on chromosome 2; therefore, the "empty" *attP* line (VDRC #60100) was used as a negative control. *UAS-dsMCO1b* was inserted at random via a *P*-element mediated event, and w^{1118} (VDRC #60000) was used as the negative control. For experiments that required the genotypic identification of larval progeny from

heterozygous parents, a GFP-marked *CyO* balancer chromosome was used (BDSC #4523).

RNA isolation and quantitative RT-PCR

Total RNA was isolated using the Tri reagent method (Sigma), and genomic DNA was removed with DNAseI. The quality of DNAse-treated total RNA was verified with a Bioanalyzer (Agilent). Pools of cDNA were synthesized with the SuperScript First-Strand Synthesis System for RT-PCR (Invitrogen) with oligo(dT) primers. Real-time PCR reactions were monitored on an iCycler (Bio-Rad) by means of SYBR Green (Bio-Rad) dye. Expression data were normalized to *ribosomal protein 49* (*rp49*) or *glyceraldehyde 3-phosphate dehydrogenase* (*gapdh*) expression. Primers are listed in Table S2. Pairwise differences in expression were assessed by performing an unpaired *t* test, multiple comparisons were analyzed by one-way ANOVA followed by Dunnett's test (or Tukey's test for data sets of n = 2). All statistical analyses were performed with GraphPad Prism software.

Production of polyclonal antiserum and immunoblot analysis

Polyclonal antiserum was generated against residues Asp346 - Asp691 of mature MCO1 (Figure S2) using methods described previously [27] with minor modifications. Excised gel slices containing the recombinant protein were sent to Open Biosystems (Rockford, Illinois) for the production of polyclonal antiserum in a rabbit. To remove antibodies that might react with conserved epitopes in other multicopper oxidases, the antiserum was incubated with purified *A. gambiae* MCO4 [19], and the unbound fraction was retained.

Immunohistochemistry

To detect MCO1 in midguts, immunostaining of cryosections was performed as described previously [27] with minor modifications. Briefly, dissected guts from wandering larvae or adult females were fixed in 4% paraformaldehyde in phosphate buffered saline (PBS) for 1 h, sections were incubated for 2 h with partially purified MCO1 antiserum or pre-immune serum, and Alexa Fluor 488 conjugated goat anti-rabbit IgG (Invitrogen) was used as the secondary antibody. To detect MCO1 in whole tissues, the digestive system plus Malpighian tubules were fixed with 4% paraformaldehyde in PBS for 2 h, permeabilized in PBS-Triton (PBS + 1.5% Triton X-100) for 5 min, and blocked for 1 h in PBS + 1% Triton X-100 + 5% bovine serum albumin. Tissues were incubated with partially purified MCO1 antiserum (1:200 - 1:1000) or pre-immune serum for 24 h at 4^{o}C, washed with PBS-Triton buffer for 24 h at 4°C, incubated in Alexa Fluor 488 conjugated goat anti-rabbit IgG (Invitrogen, 1:500) for 24 h at 4°C, washed with PBS for 24 h at 4°C, stained with DAPI for 15 min, and washed with PBS overnight at 4°C. Sections and tissues were analyzed with a Zeiss LSM 510 META laser scanning confocal microscope using excitation wavelengths of 405 and 488 nm and a 10× Plan-Neofluar objective with a 0.3 numerical aperture or a 40× Plan-Neofluar oil objective with a 1.3 numerical aperture. The specificity of MCO1 immunoreactivity was verified by immunostaining tissues from MCO1 knockdown insects (Figure S4).

Longevity assay

Female *da-Gal4* flies were crossed with *UAS-dsMCO1a*/ *CyO* or *attP* males. Progeny were cultured on unsupplemented food. Within one day after eclosion, control (*da-Gal4>attP*) and MCO1 knockdown (*da-Gal4>UAS-dsMCO1a*) female and male flies were selected and raised on food supplemented with 0 or 10 mM ferric ammonium citrate. Twenty-five flies were placed in a vial with food. Flies were cultured at 25°C and transferred to vials with fresh food every 2–3 days. Dead flies were counted every 24 h. Four to six biological replicates were done. Survival curves were compared by performing a log-rank (Mantel-Cox) test with the use of GraphPad Prism software.

Histological staining of iron in midgut cells

For detecting iron in the iron-storing cells of the midgut [35], a Prussian blue staining method was used [29]. Midguts from wandering larvae or female adults were dissected and fixed in 4% formaldehyde, permeabilized with 1% Tween-20, incubated with 2% $K_4Fe(CN)_6$ in 2% HCl, and rinsed with water. Larvae were cultured on regular food; newly eclosed adults were transferred to food supplemented with 1 mM ferric ammonium citrate for one day (for the purpose of increasing the amount of iron in the midgut to reliably detectable levels) and then transferred to regular food for 24 h to clear the high iron food from the gut lumen. Images were taken with a Zeiss Axio Imager microscope with a 10× objective and AxioCam camera. At least eight midguts of each genotype were analyzed. AxioVision software was used to outline the blue region of each midgut and to calculate the areas. Differences in areas were assessed by performing a Mann Whitney test (for data sets with unequal variance) or an unpaired *t* test using GraphPad Prism software.

Ferrozine-based assay

For estimating whole body iron concentrations, we used a ferrozine-based assay that has been described previously [30]. Heads were removed from adults to avoid potential interference from eye pigments. Adults were cultured for five days on food supplemented with 10 mM ferric ammonium citrate to mimic the conditions used in the longevity experiment and then tranfered to regular food for 24 h to clear the high iron food from the gut lumen. We homogenized 13 wandering larvae or 10 female adults in 135 µl of lysis buffer (20 mM Tris, 137 mM NaCl, 1% Triton X-100, 1% glycerol). Samples were centrifuged to remove insoluble material. For blank controls, we substituted lysis buffer for the soluble fraction. Protein concentration was determined with a Bradford assay. Proteins were hydrolyzed with concentrated hydrochloric acid at 95°C, and ferric iron was reduced to ferrous iron with ascorbate. Ferrozine was added to the samples, and the pH was increased with the addition of ammonium acetate. Complex formation was detected by absorbance at 562 nm. The concentration of iron was calculated based on a molar extinction coefficient of the iron-ferrozine complex of

27,900 M^{-1} cm^{-1} [36]. Three biological replicates were performed, and differences in iron concentration were assessed by performing an unpaired *t* test using GraphPad Prism software.

Acknowledgements

We thank Neal Dittmer, Yoonseong Park, Lawrence Davis, Ramaswamy Krishnamoorthi and Karl Kramer for helpful suggestions regarding this work. We thank Stewart Gardner for his technical assistance. We thank Joel Sanneman for training and help with cryosectioning and confocal microscopy, and we thank Philine Wangemann for advice and the use of the Center of Biomedical Research Excellence (COBRE) Confocal Microfluorometry and Microscopy Core Facility. We thank the Integrated Genomics Facility at Kansas State University for training and advice regarding real time PCR. This work was supported by Grant Number R01AI070864 from the National Institute of Allergy and Infectious Diseases. The COBRE Confocal Microfluorometry and Microscopy Core Facility is supported by Kansas State University and the National Institutes of Health Grant P20-RR017686. This is contribution 12-382-J from the Kansas Agricultural Experiment Station.

References

1. Kosman D (2010) Redox cycling in iron uptake, efflux, and trafficking. J Biol Chem 284:711-715.

2. Philpott CC, Protchenko O (2008) Response to iron deprivation in *Saccharomyces cerevisiae*. Eukaryotic Cell 7:20-27.

3. Terzulli A, Kosman DJ (2010) Analysis of the high-affinity iron uptake system at the *Chlamydomonas reinhardtii* plasma membrane. Eukaryotic Cell 9:815-826.

4. De Domenico I, et al. (2007) Ferroxidase activity is required for the stability of cell surface ferroportin in cells expressing GPI-ceruloplasmin. EMBO J 26:2823-2831.

5. Han O (2011) Molecular mechanisms of intestinal iron absorption. Metallomics 3:103-109.

6. Petrak J, Vyoral D (2005) Hephaestin - a ferroxidase of cellular iron export. Int J Biochem Cell Biol 37:173-1178.

7. Hellman NE, Gitlin JD (2002) Ceruloplasmin metabolism and function. Annu Rev Nutr 22:39-458.

8. Bettedi L, Aslam MF, Szular J, Mandilaras K, Missirlis F (2011) Iron depletion in the intestines of *Malvolio* mutant flies does not occur in the absence of a multicopper oxidase. J Exp Biol 214:971-978.

9. Pham DQD, Winzerling JJ (2010) Insect ferritins: typical or atypical. Biochim Biophys Acta 1800:824-833.

10. Huebers HA, et al. (1988) Iron binding proteins and their roles in the tobacco hornworm, *Manduca sexta* (L.). J Comp Physiol B 158:291-300.

11. Bartfeld NS, Law JH (1990) Isolation and cloning of transferrin from the tobacco hornworm, *Manduca sexta*: sequence similarity to the vertebrate transferrins. J Biol Chem 265:21684-21691.

12. Geiser DL, Winzerling JJ (2012) Insect transferrins: multifunctional proteins. Biochim Biophys Acta 1820:437-451.

13. Huston WM, Jennings MP, McEwan AG (2002) The multicopper oxidase of *Pseudomonas aeruginosa* is a ferroxidase with a central role in iron acquisition. Mol Microbiol 45:1741-1750.

14. Hoopes JT, Dean JFD (2004) Ferroxidase activity in a laccase-like multicopper oxidase from *Liriodendron tulipifera*. Plant Physiol Biochem 42:27-33.

15. Dittmer NT, Kanost MR (2010) Insect multicopper oxidases: diversity, properties, and physiological roles. Insect Biochem Mol Biol 40:179-188.

16. Sakurai T, Kataoka K (2007) Basic and applied features of multicopper oxidases, CueO, bilirubin oxidase, and laccase. Chem Rec 7:20-229.

17. Graveley BR, et al. (2011) The developmental transcriptome of *Drosophila melanogaster*. Nature 471:473-479.

18. Chintapalli VR, Wang J, Dow JAT (2007) Using FlyAtlas to identify better *Drosophila melanogaster* models of human disease. Nat Genet 39:715-720.

19. Gorman MJ, Dittmer NT, Marshall JL, Kanost MR (2008) Characterization of the multicopper oxidase gene family in *Anopheles gambiae*. Insect Biochem Mol Biol 38:817-824.

20. Baker DA, et al. (2011) A comprehensive gene expression atlas of sex- and tissue-specificity in the malaria mosquito, *Anopheles gambiae*. BMC Genomics 12:296.

21. Dittmer, NT et al. (2004) Characterization of cDNAs encoding putative laccase-like multicopper oxidases and developmental expression in the tobacco hornworm, *Manduca sexta*, and the malaria mosquito, *Anopheles gambiae*. Insect Biochem Mol Biol 34:29-41.

22. Zhukhlistova NE, Zhukova YN, Lyashenko AV, Zaitsev VN, Mikhailov AM (2008) Three-dimensional organization of three-domain copper oxidases: a review. Crystallogr Rep 53:2-109.

23. Taylor AB, Stoj CS, Ziegler L, Kosman DJ, Hart PJ (2005) The copper-iron connection in biology: structure of the metallo-oxidase Fet3p. Proc Natl Acad Sci USA 102:15459-15464.

24. Quintanar L, et al. (2007) Shall we dance? How a multicopper oxidase chooses its electron transfer partner. Acc Chem Res 40:445-452.

25. Stoj CS, Augustine AJ, Zeigler L, Solomon EI, Kosman DJ (2006) Structural basis of the ferrous iron specificity of the yeast ferroxidase, Fet3p. Biochemistry 45:12741-12749.

26. Gorman MJ, et al. (2012). Kinetic properties of alternatively spliced isoforms of laccase-2 from *Tribolium castaneum* and *Anopheles gambiae*. Insect Biochem Mol Biol 42:193-202.

27. Lang M, Kanost MR, Gorman MJ (2012) Multicopper oxidase-3 is a laccase associated with the peritrophic matrix of *Anopheles gambiae*. PLoS One 7:e33985.

28. Chen H et al. (2004) Hephaestin is a ferroxidase that maintains partial activity in sex-linked anemia mice. Bood 103:3933-3939.

29. Mehta A, Deshpande A, Bettedi L, Missirlis F (2009) Ferritin accumulation under iron scarcity in *Drosophila* iron cells. Biochimie 91:1331-1334.

30. Missirlis F., et al. (2006) Characterization of mitochondrial ferritin in *Drosophila*. Proc Natl Acad Sci USA 103:5893-5898.

31. Gkouvatsos K, Papanikolaou G, Pantopoulos K (2012) Regulation of iron transport and the role of transferrin. Biochim Biophys Acta 1820:188-202.

32. Ong ST, Ho JZS, Ho B, Ding JL (2006) Iron-withholding strategy in innate immunity. Immunobiology 211:295-314.

33. De Gregorio E, Spellman PT, Rubin GM, Lemaitre B (2001) Genome-wide analysis of the *Drosophila* immune response by using oligonucleotide microarrays. Proc Natl Acad. Sci USA 98:12590-12595.

34. Tiklova K, Senti KA, Wang S, Graslund A, Samakovlis C (2010) Epithelial septate junction assembly relies on melanotransferrin iron binding and endocytosis in *Drosophila*. Nat Cell Biol 12:1071-1077.

35. Poulson DF (1950) Chemical differentiation of the larval mid gut of *Drosophila*. Genetics 35:130-131.

36. Stookey LL (1970) Ferrozine - a new spectrophotometric reagent for iron. Anal Chem 42:779-781.

Figure legends

Figure 1. Ferroxidase activity of MCO1. MCO1 and two mosquito laccases, MCO2A and MCO3, were analyzed by triplicate native gels. A) Coomassie staining. B) Activity assay using *p*-phenylenediamine, a substrate of laccases and multicopper ferroxidases [28]. C) Assay for ferroxidase activity using ferrous ammonium sulfate as the substrate. Note that all of the enzymes oxidized *p*-phenylenediamine but only MCO1 had detectable ferroxidase activity.

Figure 2. Immunolocalization of MCO1. Cryosections of larval (A) and adult (B) midguts and unsectioned larval (C) and adult (D) Malpighian tubules were immunostained with MCO1 antiserum. Anti-MCO1 antibodies were detected with Alexa Fluor 488 conjugated anti-rabbit IgG antibodies (green). Nuclei were stained with DAPI (blue). Immunoreactivity was detected along the basal surface of the epithelial cells of the midgut and Malpighian tubules. Scale bars represent 10 μm.

Figure 3. Effect of MCO1 knockdown on longevity. Female (A) and male (B) flies were cultured on regular food or food supplemented with 10 mM ferric ammonium citrate (Fe). Longevity of MCO1 knockdown flies (KD) and control flies (C) was similar when the flies were fed normal food (gray and red curves). Flies cultured on food supplemented with 10 mM iron (blue and green curves) had decreased longevity compared with flies fed regular diet ($P < 0.0001$ for females and males), demonstrating that 10 mM iron was toxic to the flies. Most importantly, MCO1 knockdown flies lived longer than control flies when they were fed the high iron diet (green versus blue curves, $P < 0.0001$ for females and males). Knockdown genotype = *da-Gal4>UAS-dsMCO1a*; control genotype = *da-Gal4>attP*. Data are from at least four biological replicates. Standard errors are shown. Survival curves were compared by performing a log-rank (Mantel-Cox) test. (Note that in panel A, the gray and red curves overlap.)

Figure 4. Effect of MCO1 knockdown on iron accumulation in the midgut. Midguts of control (C) and knockdown (KD) genotypes were stained to detect iron. Panels A and C show the iron cell region of a representative larval midgut from control (*act-Gal4>attP*) and knockdown (*act-Gal4>UAS-dsMCO1a*) genotypes. Panels B and D show the iron cell region of a representative adult midgut from control (*da-Gal4>attP*) and knockdown (*da-Gal4>UAS-dsMCO1a*) genotypes. The scale bars represent 100 μm. Knockdown was correlated with a reduction in the blue area of the midguts (E = larva, F = adult). Number of midguts analyzed: *act-Gal4>attP*, n = 21; *act-Gal4>UAS-dsMCO1a*, n = 23; *da-Gal4>attP*, n = 8; and *da-Gal4>UAS-dsMCO1a*, n = 8. Means ± standard deviations are shown. Differences in areas were assessed by performing a Mann Whitney test (E) or unpaired *t* test (F). (** = $P < 0.01$, **** = $P < 0.0001$.)

Figure 5. Effect of MCO1 knockdown on iron accumulation in whole insects. A ferrozine-based assay was used to determine the concentration of iron in whole larvae cultured on regular food (A) and adult females cultured on food supplemented with 10 mM ferric ammonium citrate (B). At both life stages, knockdown insects had less iron than controls. Larval genotypes were *act-Gal4>attP* (C) and *act-Gal4>UAS-dsMCO1a*

(KD); adult genotypes were *da-Gal4>attP* (C) and *da-Gal4>UAS-dsMCO1a* (KD). Data are from three biological replicates. Means ± standard deviations are shown. Differences in iron content were assessed by performing an unpaired *t* test. (* = $P < 0.05$, ** = $P < 0.01$.)

Figure 6. Effect of MCO1 knockdown on the expression of the iron importer DMT1. Quantitative RT-PCR was used to analyze *DMT1* expression in the midguts of control and knockdown larvae (A) and adults (B). Knockdown of MCO1 resulted in a decrease in *DMT1* transcript abundance in the midgut. Larval genotypes were *act-Gal4>attP* (C) and *act-Gal4>UAS-dsMCO1a* (KD); adult genotypes were *da-Gal4>attP* (C) and *da-Gal4>UAS-dsMCO1a* (KD). Data were normalized to *rp49* expression. Data are from three biological replicates. Means ± standard deviations are shown. Differences in expression were assessed by performing an unpaired *t* test. (* = $P<0.05$, ** = $P < 0.01$.)

Table 1. Catalytic efficiencies of MCO1 and two insect laccases

Substrate	**MCO1**[a]	**MCO2A**[a,b]	**MCO3**[a,b]
hydroquinone	6	114	302
dopamine	2	96	171
NADA	activity not detected	307	155
NBAD	12	219	323

[a]Catalytic efficiencies (k_{cat}/ K_m) are in min^{-1} mM^{-1}.
[b]The catalytic efficiencies of MCO2A and MCO3 were reported previously [26, 27].

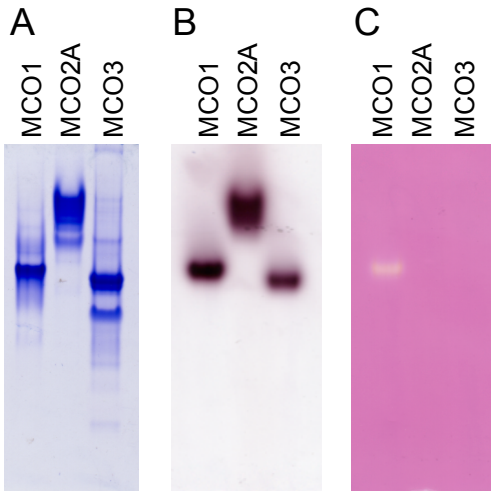

Figure 1

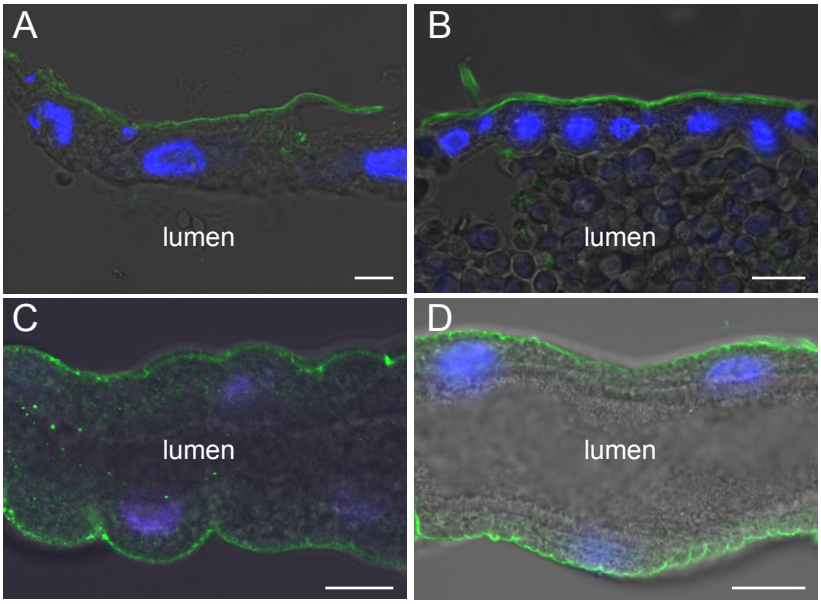

Figure 2

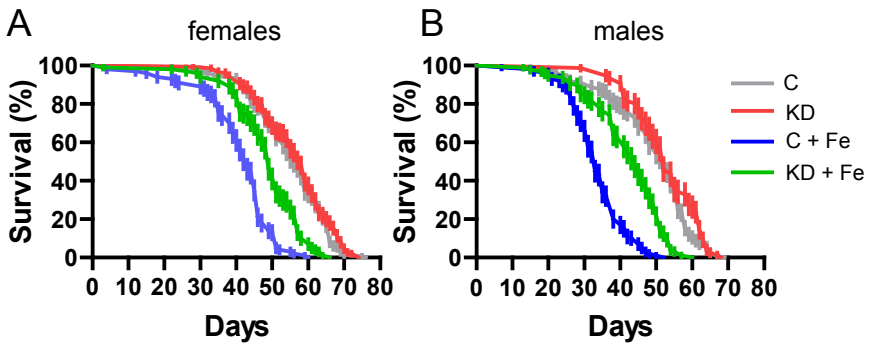
A
females
B
males
Survival (%)
100
80
60
40
20
0
0 10 20 30 40 50 60 70 80
Days
C
KD
C + Fe
KD + Fe

Figure 3

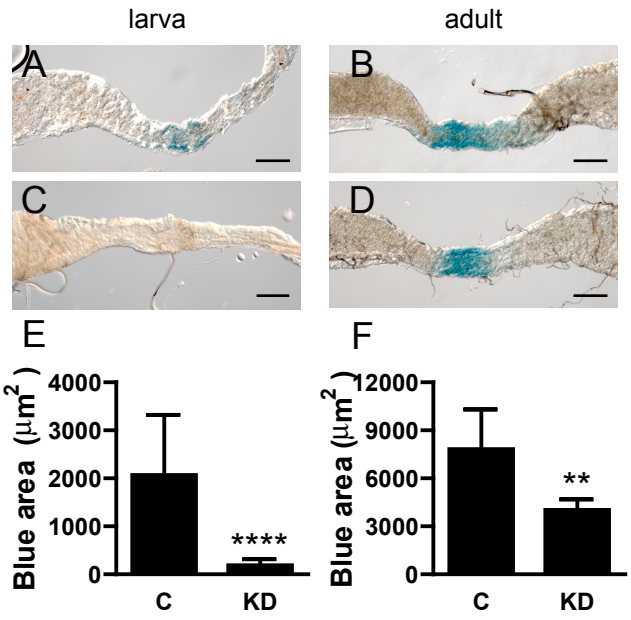
larva
adult
A
B
C
D
E
F
Blue area (μm²)
4000
3000
2000
1000
0
****
C
KD
Blue area (μm²)
12000
9000
6000
3000
0
**
C
KD

Figure 4

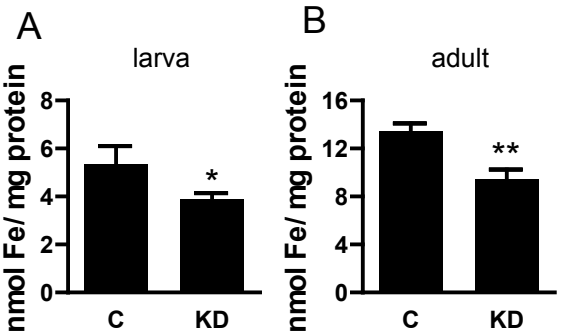
A
larva
nmol Fe/ mg protein
8
6
4
2
0
*
C
KD
B
adult
nmol Fe/ mg protein
16
12
8
4
0
**
C
KD

Figure 5

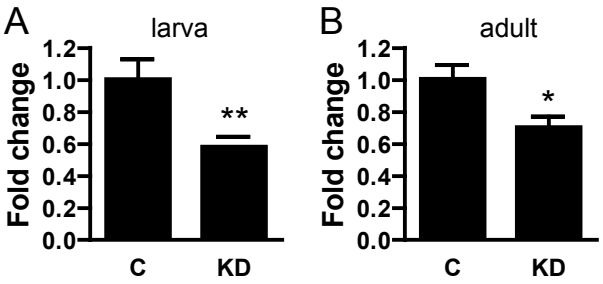
A
larva
Fold change
1.2
1.0
0.8
0.6
0.4
0.2
0.0
**
C
KD
B
adult
Fold change
1.2
1.0
0.8
0.6
0.4
0.2
0.0
*
C
KD

Figure 6

Figure S1. Amino acid sequence alignments. An analysis of sequence alignments indicated the presence of two putative iron binding residues in DmMCO1. A) Alignment of DmMCO1 and Fet3p. Residues highlighted in magenta are known (Fet3p) or predicted (DmMCO1) iron binding residues. Residues highlighted in yellow are known (Fet3p) or predicted (DmMCO1) copper binding residues. Non-alignable sequences at the amino- and carboxyl-termini were omitted from the alignment. B) Alignment of partial insect MCO sequences. Alignments demonstrate conservation of the two putative iron binding residues in MCO1 sequences (highlighted in magenta). Species names and GenBank IDs are listed in Table S1.

Figure S2. Amino acid sequence, SDS-PAGE and immunoblot analysis of purified recombinant MCO1. A) Amino acid sequence of MCO1. The predicted signal peptide is indicated by gray highlighting of white text. The von Willebrand factor domains, cysteine-rich region, and cupredoxin-like domains I, II and III are in green, purple, red, blue and orange text, respectively. A putative carboxyl-terminal transmembrane segment is indicated by gray highlighting of black text. The 10 histidines and 1 cysteine that are predicted to bind copper are highlighted in yellow. The putative iron binding residues are highlighted in magenta. Arg454 (which was mutated to Ala454 in the recombinant enzyme) is highlighted in cyan. The region of MCO1 that was expressed as a recombinant enzyme is underlined (including double underlined region). The region of MCO1 that was used to generate polyclonal antiserum is double underlined. B) Coomassie staining was used to detect 0.8 μg of purified enzyme. C) The identity of the purified protein was verified by immunoblot analysis.

Figure S3. *MCO1* expression. Quantitative RT-PCR was used to analyze *MCO1* expression in adult female whole flies (A, B) midguts (C) and Malpighian tubules (D). Flies were fed for one (A) or seven (B-D) days on food supplemented with 0 (control), 0.5 or 10 mM ferric ammonium citrate. Iron supplementation had no detectable effect on *MCO1* expression. Data are from three biological replicates and were normalized to *gapdh* expression. Means ± standard deviations are shown. Differences in means were assessed by performing one-way ANOVA followed by Dunnett's test (A, B) or by performing an unpaired *t* test (C, D). Abbreviations: mg = midgut, Mt = Malpighian tubules.

Figure S4. Verification of MCO1 immunolocalization. Immunostaining was performed to assess localization of MCO1 along the length of the adult digestive system and Malpighian tubules (A) and to verify the specificity the MCO1 antiserum (B-I). Whole adult digestive systems plus Malpighian tubules (A), cryosections of larval (B, C) and adult (D, E) midguts, and unsectioned larval (F, G) and adult (H, I) Malpighian tubules were analyzed. Control genotypes were *act-Gal4>attP* (B, D, F, H); MCO1 knockdown genotypes were *act-Gal4>UAS-dsMCO1a* (C, G), *da-Gal4>UAS-dsMCO1a* (E) or *act-Gal4>UAS-dsMCO1b* (I). Little or no staining of tissues from knockdown insects was observed. No immunoreactivity to basal surfaces was observed when tissues were incubated with preimmune serum, but small spots in the lumen of the midgut or Malpighian tubule were sometimes observed (similar to those in (E)). Anti-MCO1 antibodies were detected with Alexa Fluor 488 conjugated anti-rabbit IgG antibodies

(green). Nuclei were stained with DAPI (blue, not shown in A). Scale bar in A = 500 μm; scale bars in B-I = 10 μm. Abbreviations: mg = midgut, Mt = Malpighian tubules.

Figure S5. Verification of RNAi-mediated MCO1 knockdown. Quantitative RT-PCR was used to analyze *MCO1* expression in control and MCO1 knockdown flies. A) Strong knockdown using an *actin-Gal4* driver line was verified in wandering larvae. Data were normalized to *rp49* expression. Data are from three biological replicates. Means ± standard deviations are shown. Differences in expression between knockdown and control genotypes were assessed by performing one-way ANOVA followed by Dunnett's multiple comparison test. B) Weak knockdown using a *daughterless-Gal4* driver line was verified in adult females. Data were normalized to *rp49* expression. Data are from two biological replicates. Means ± standard deviations are shown. Differences in expression between knockdown and control genotypes were assessed by performing one-way ANOVA followed by Tukey's test. (* = $P < 0.05$.)

Figure S6. Verification of RNAi phenotypes. An independent MCO1 RNAi line, *UAS-dsMCO1b*, was used to verify the correlation between MCO1 knockdown and decreased iron accumulation. A) Midguts of control (C) and knockdown (KD) larvae were stained to detect iron in the iron cells, and the blue pigmented area of each midgut was determined. Knockdown was correlated with a reduction in the blue areas. Control genotype = *mg+sg-Gal4>+*; knockdown genotype = *mg+sg-Gal4>UAS-dsMCO1b*. Means ± standard deviations are shown, n = 11. Differences in areas were assessed by performing a Mann Whitney test. (*** = $P<0.001$.) B) A ferrozine-based assay was used to determine the concentration of iron in newly eclosed whole adult females (cultured as larvae on food supplemented with 10 mM ferric ammonium citrate). Knockdown (KD) insects had less iron than controls (C). Control genotype = *act-Gal4>+*; knockdown genotype = *act-Gal4>UAS-dsMCO1b*. Data are from three biological replicates. Means ± standard deviations are shown. Differences in iron content were assessed by performing an unpaired t test. (* = $P<0.05$.)

Table S1. GenBank IDs of sequences used for alignments

Species	**Phylogenetic group**[a]	**GenBank ID**
Drosophila melanogaster	MCO1	NM_135443
D. melanogaster	MCO2	NM_165431
D. melanogaster	MCO3	NM_135443
D. melanogaster	MCO4	NM_133021
Anopheles gambiae	MCO1	AY135184
A. gambiae	MCO2	AY943928
A. gambiae	MCO3	EF592176
A. gambiae	MCO4	EU380796
A. gambiae	MCO5	EU380797
Aedes aegypti	MCO1	XM_001652867
Culex quinquefaciatus	MCO1	XP_001862911
Manduca sexta	MCO1	AY135185
M. sexta	MCO2	AY135186
Bombyx mori	MCO1	BK006377
Tribolium castaneum	MCO1	AY884065
T. castaneum	MCO2	AY884061
Apis mellifera	MCO1	XM_001120790
A. mellifera	MCO2	XM_393845
A. mellifera	MCO3	XM_625186
Acyrthosiphon pisum	MCO1	XP_001948070
A. pisum	MCO2	XP_001950788
Pediculus humanus	MCO1	XP_002422943.1
Saccharomyces cerevisiae	Fet3p	NP_013774.1

[a]The designations MCO1 and MCO2 refer to orthologous groups, but the designations MCO3 and MCO4 do not.

Table S2. Primers used for real-time PCR

Gene name	Primer sequence (Forward)	Primer sequence (Reverse)
MCO1[a]	5'-CTGGATAATGGACAGATTG-3'	5'-AGTAGGGACAACAGTTTC-3'
MCO1[b]	5'-CGGAAGCGGACTACAAGTTC-3'	5'-GCGACAATCGATACCCTGAT-3'
DMT1	5'-GCCTTGGTTAAGTCCCG-3'	5'-GCCATACATGCCATGGGC-3'
rp49	5'-TACAGGCCCAAGATCGTGAA-3'	5'-TCTCCTTGCGCTTCTTGGA-3'
gadph[c]	5'-CGTTCATGCCACCACCGCTA-3'	5'-CCACGTCCATCACGCCACAA-3'

[a]MCO1 primers used for experiment described in Figure S5, panel B.
[b]MCO1 primers used for experiment described in Figures S3 and S5, panel A.
[c]Ling D, Salvaterra, PM (2011) Robust RT-pPCR data normalization: validation and selection of internal reference genes during post-experimental data analysis. PLoS One 6:e17762

A

```
DmMCO1 VMDGLERSITVVNRMMPGPAIEVCEGDEIVVDVKNHLLGESTSIHWHGLHQKKTPYMDGVPHITQCPITPHATFRYSFPADLSG-THFWHSHTGM
ScFet3 VDGLKSRPVITCNGQFPWPDITVNKGDRVQIYLTNGMNNTNTSMHFHGLFQNGTASMDGVPFLTQCPIAPGSTMLYNFTVDYNVGTYWYHSHTDG
       * .  .*.: . *  :* * * * :**.: : :.* : . .**:*:***.*: *. *****.:*****:* :*: *.*..* .  *:::****.

DmMCO1 QRGDGVFGALIIRKPKTAEPHGGLYDFDLSEHVMIVQDWIHDTGASIFSYHHHSRGDNKPHNLLVNGKGRYYNRIWAEAKQAHRRAEERTTQPVE
ScFet3 QYEDGMKGLFIIKDDSFPYDYDEELSLSLSEWY---HDLVTDLTKSFMSVYNPTGAEPIPQNLIVNN----------------------------
       *  **: * :**:. . .  :.   .:.***     :* : *   *::* :: : .:  *:**:**.

DmMCO1 PLPKSQVDFVQTLPRQARLAKTNTTKLFPVNSRQKRGNLNEIPLELVPHQIVTYSGERFDFVLNANLEVGNYWIRLKGLMD-CSEVFTSAFQVAI
ScFet3 ---------------------------------------------TMNLLYITVAQRYTVLVHTKNDTDKNFAIMQKFDDTMLEVIPSDLQLNA
                                                     . : :    .:*: .::::: :..: :  :: : *   :*:.* :*:

DmMCO1 LRYEGAPDEEPTAELSYGHKAEGIELNVMNRGPGYPDTKTVAEMRALPIYDHVSGIDHDTLKPEADYKFFIYYDFYTKNNPDFHDKDLYAMDMEM
ScFet3 TSYMVYN---KTAALPTQNYVDSIDN---FLDDFYLQPYEKEAIYGEPDHVITVDVVMDNLKNGVNYAFFNNITYTAPKVP--------------
         *        ** *.  : .:.*:      .  * :.    : . * :  . .:  *.**  .:* **    : : : *

DmMCO1 TQQNRLYTPQLNHITLNFPSLALLPSRSQLKDSDFCNETSLMDQGIDCRQEFCKCHHVLQVPLGAVVEMIIVDEGFQYYANHPFHLHGNAFRVMG
ScFet3 ------------------TLMTVLSSGDQANNSEIYGSN----------------THTFILEKDEIVEIVLNNQ---DTGTHPFHLHGHAFQTIQ
                       . :::*.* .* ::*:: ...                 *.: :  . :**::: ::     ..*******:**:.:

DmMCO1 LERLGENVTVEMIKQLDQFNLLKRNLDNPPVKDTVTIPDGGYTIIRFEASNPGYWLFHCHIEFHAEIGMALVFKVG----NDDQMVPVPENFPTC
ScFet3 RDRTYDDALGEVPHSFDPDNHP-AFPEYPMRRDTLYVRPQSNFVIRFKADNPGVWFFHCHIEWHLLQGLGLVLVEDPFGIQDAHSQQLSENHLEV
        :*  ::.  *: :.:*  *      : *  :**: :   .  :***:*.*** *:******:*   *:.**:  .    :* :   :.**.
```

B

```
DmMCO1  DWIHDTGASIFSYHHHSRGD-NKPHNLLVNGKG    YWIRLKGLMDCSEVFTSAFQVAILRY
AgMCO1  DWGHEQGVSLFASHHHSTGD-NKPPNLLINGRG    YLIRFRGLMDCDERFTSAYQFAVLRY
AaMCO1  DWGHVAGNQMFTAHHHSTGD-NKPPNILINGRG    YLMRFRGLMDCDERFTSAYQVAVLRY
CqMCO1  DWGHEAGVQMFVAHHHSIGD-NKPPNILVNGRG    YLMRFRGLMDCDERFTSAYQVAVLRY
MsMCO1  DWIHQLAVGMFTDHHHSSGD-NKPPTLLINGVG    YWIRFRGLMDCDEIYTRAKQVAVLHY
BmMCO1  DWIHELSVGMFTDHHHSSGD-NKPPTLLINGVG    YWIRFRGLMDCDEVFTKAKQVGVLHY
TcMCO1  DWTKEDGTDKFMSHIHNDGD-NKPDTILVNGFG    YWMHFRGLMDCDERFTRAYQVAVLEY
AmMCO1  DWTHELGIDKFLNHHYAGGD-NKPPNILINGLG    FWIRFRGLMDCDERFTKAYQVAILRY
ApMCO1  DWLHELGIRKFLAHYHGSGN-NKPETILINGRG    YWMRFRGLMDCDERFTKAFEVSILHY
PhMCO1  DWTHTFSADKFSLHIHGAKD-NQPSTLLINGKG    YWIRFKGLLDC--KFKEAYQTAILHY
DmMCO2  DWLHEDAAERYPGRLAVNTG-QDPESMLINGKG    YWIQLRGLGECG--IRRAQQLAILRY
AgMCO2  DWLHEDAAERYPGRLAVNTG-QDPESLLINGKG    YWIQLRGLGECG--IKRAQQLAILRY
MsMCO2  DWLHDDAAERYPGRLAVNTG-QDPESVLINGKG    YWIQVRGLGECG--IKRAQQLGILRY
TcMCO2  DWMHEDATERFPGRLAVNTG-QDPESLLINGKG    YWIQLRGLGECG--IRRVQQLGILRY
AmMCO2  DWFHENAAERFPGRLAVNTG-QAPESVLINGKG    YWIQVRSLGECG--IPRAQQLGILRY
ApMCO2  DWLHENGMERFPGRLAANTG-QDPESLLINGKG    YWIQVRGLGECG--NKRVQQLAILRY
AgMCO3  DWMRIDGEMFMPG-LPSAGG-IMPINLLINGKG    YWVRLRSLGPCA--DLQLEQFAVLRY
AgMCO4  DWTLDLVEKFVPGLQSSTV---RMDSILINGRG    YWVRVRAIGFCN--IERREEFAVLSY
AgMCO5  DWTLDMVEKWVPGIQTDSM---RVDSILINGRG    YWVRVRGIGFCD--QMRVEDFAILSY
DmMCO3  DIFYEYNL-------------QDVRNILVNGKG    YWIRIKGYEQCE--NRNIYQGAVLSY
DmMCO4  DWVHNFVESVA----------ENILINGRG       YWIRVKGYSFCA--KNQLHQEAVLHY
AmMCO3  DWIHELSFERYPGYYRYNVLGQTAENILINGLG    YWIQARGLGECA--TTFMQQLAILKY
        *                        .:*:** *    : :: :.   *        : .:* *
```

Figure S1

A

MPVVNSRLAELARITVLLTALLVSYASGLQTVGESADDNTICLYREYNTTYRKEIGAVWFASKDPCLVYSCAAGVAKDPQA
HIVATQVDCNEFYCEVGSELRSVEGSCCGECVRTHCQHNHTLYAVGESWHNDADCTLIECGRLDNGQIVMNTYKRNCPALT
EDCPASRLEERNCCPYCRPLQTARIEELQDNVAESTDDIWTAEWYRNHPCNRDCQVGAEPMTCRYKFVVEWYQTFSKACYD
CPRNLTDCSRPHCVMGDGLERSITVVNRMMPGPAIEVCEGDEIVVDVKNHLLGESTSIHWHGLHQKKTPYMDGVPHITQCP
ITPHATFRYSFPADLSGTHFWHSHTGMQRGDGVFGALIIRKPKTAEPHGGLYDFDLSEHVMIVQDWIHDTGASIFSYHHHS
RGDNKPHNLLVNGKGRYYNRIWAEAKQAHRRAEERTTQPVEPLPKSQVDFVQTLPRQARLAKTNTTKLFPVNSRQKRGNLN
EIPLELVPHQIYTVRRGFRYRFRIINAEYLNCPIVVSIDGHNLTAINSDGFDIEAMDVGSIVTYSGERFDFVLNANLEVGN
YWIRLKGLMDCSDVFTSAFQVAILRYEGAPDEEPTAELSYGHKAEGIELNVMNRGPGYPDTKTVAEMRALPIYDHVSGIDH
DTLKPEADYKFFIYYDFYTKNNPDFHDKDLYAMDMEMTQQNRLYTPQLNHITLNFPSLALLPSRSQLKDSDFCNETSLMDQ
GIDCRQEFCKCHHVLQVPLGAVVEMIIVDEGFQYYANHPFHLHGNAFRVMGLERLGENVTVEMIKQLDQFNLLKRNLDNPP
VKDTVTIPDGGYTIIRFEASNPGYWLFHCHIEFHAEIGMALVFKVGNDDQMVPVPENFPTCGDYNPDLRSDGGTTEDSGSS
KPITATPPNTGGGGSGLEPTWITLMISSMLVKLYR

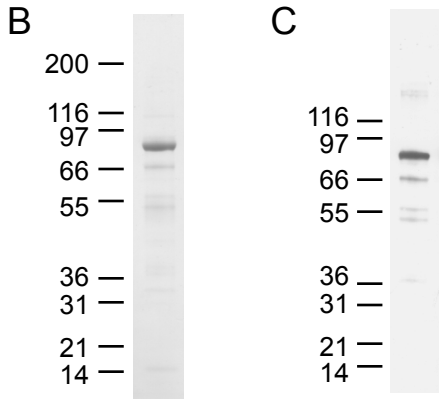

Figure S2

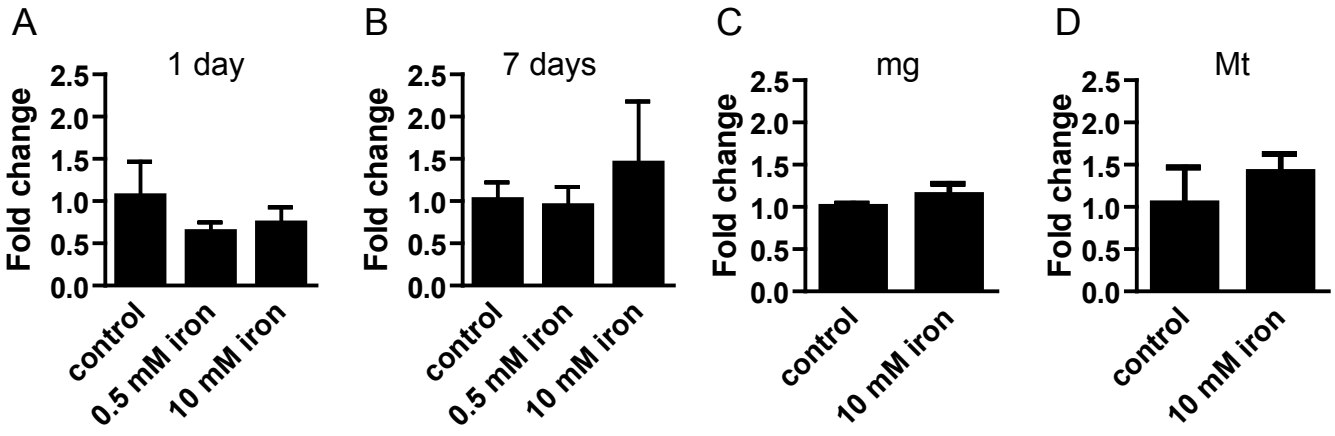
A
1 day
Fold change
2.5
2.0
1.5
1.0
0.5
0.0
control
0.5 mM iron
10 mM iron
B
7 days
Fold change
2.5
2.0
1.5
1.0
0.5
0.0
control
0.5 mM iron
10 mM iron
C
mg
Fold change
2.5
2.0
1.5
1.0
0.5
0.0
control
10 mM iron
D
Mt
Fold change
2.5
2.0
1.5
1.0
0.5
0.0
control
10 mM iron

Figure S3

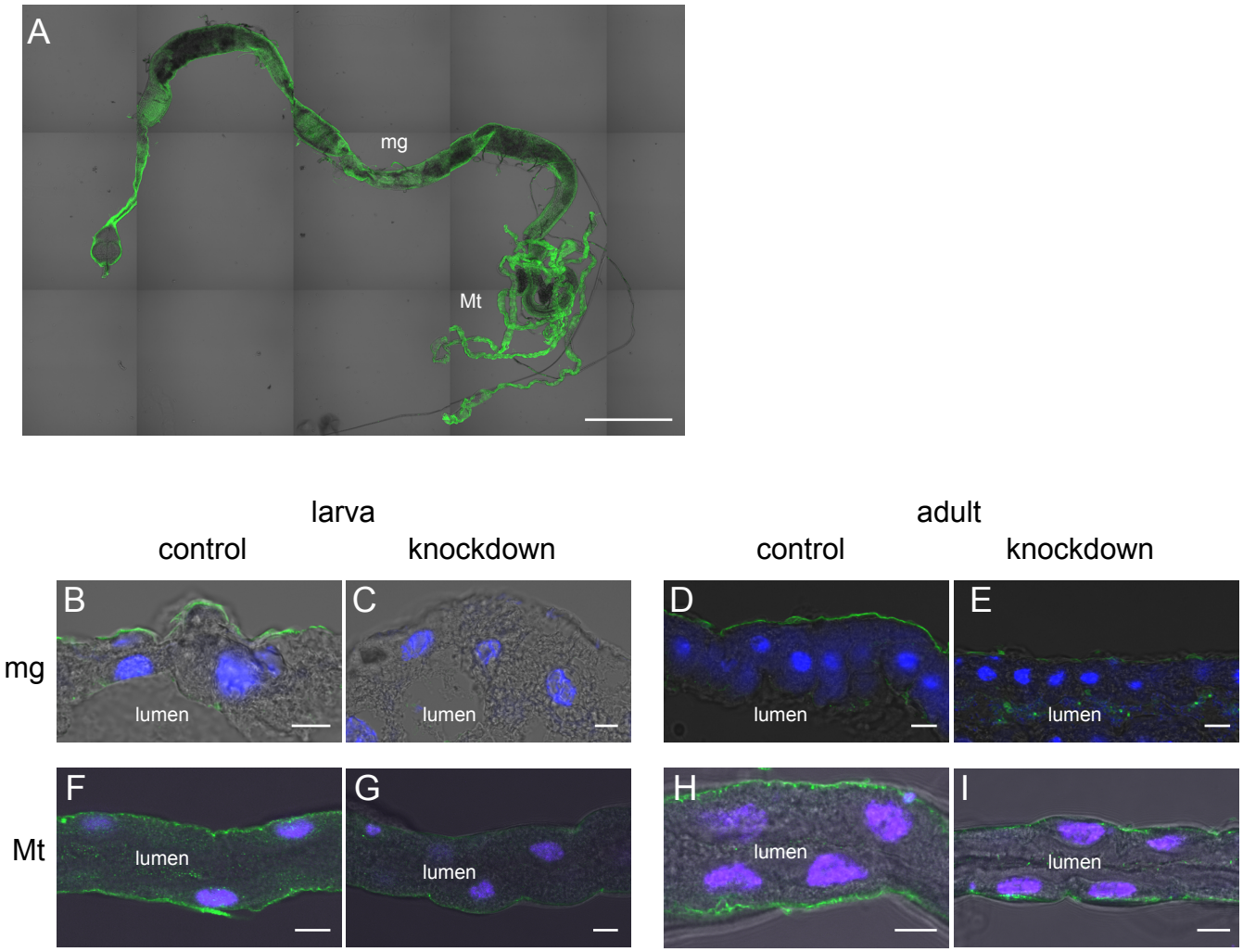
A
mg
Mt
larva
adult
control
knockdown
control
knockdown
mg
Mt
B
C
D
E
F
G
H
I
lumen

Figure S4

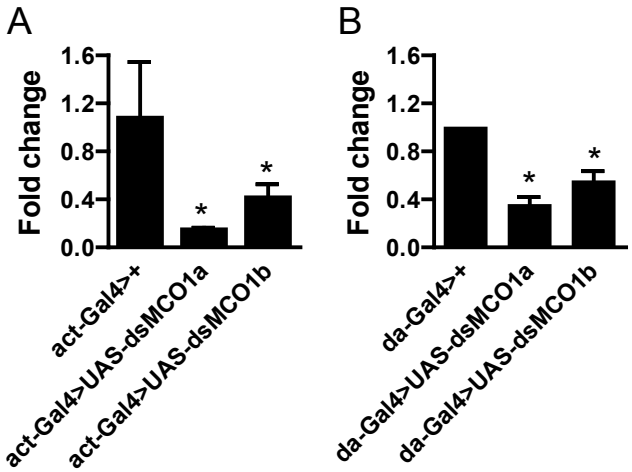
A
Fold change
1.6
1.2
0.8
0.4
0.0
*
*
act-Gal4>+
act-Gal4>UAS-dsMCO1a
act-Gal4>UAS-dsMCO1b
B
Fold change
1.6
1.2
0.8
0.4
0.0
*
*
da-Gal4>+
da-Gal4>UAS-dsMCO1a
da-Gal4>UAS-dsMCO1b

Figure S5

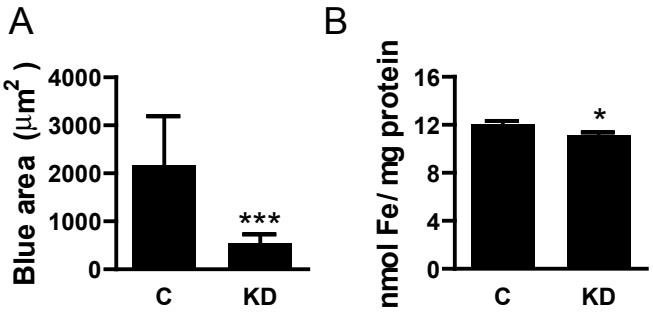
A
B
Blue area (μm²)
4000
3000
2000
1000
0
***
C
KD
nmol Fe/ mg protein
16
12
8
4
0
*
C
KD

Figure S6